

Evaluation of the interaction between SAR L-band signal and structural parameters of forest cover

Igor da Silva Narvaes; Arnaldo de Queiroz da Silva; João Roberto dos Santos
National Institute for Space Research – INPE/MCT
Av. dos Astronautas, 1758 CEP: 12.227-010 São José dos Campos, SP – Brasil
{igor,arnaldo,jroberto}@dsr.inpe.br

Abstract – The objective of this paper is to evaluate the interaction between backscatter (σ^0) from polarimetric L-band SAR data (collected by the airborne sensor R99-B/SIPAM) and biophysical parameters of the primary forest and secondary succession sites. The area under study is located in the region of Tapajós (Brazil), where SAR data were collected in May 2005. Another approach under investigation is the evaluation of the contribution from basic backscatter mechanisms, using the Freeman-Durden decomposition technique, applied to complex SAR images, where the physiognomic-structural characteristics of the forest stands give a significant contribution. In brief, it was possible to verify that the variable “tree height” has better relations with the backscatter values, when compared to other biophysical variables, especially when the model also includes variations of the incidence angle of the stripes imaged. The decomposition technique showed that the volumetric scattering component has the strongest influence on the SAR response at primary and secondary tropical forests.

Keywords: forest inventory, remote sensing, SAR, tropical forest, monitoring, Amazon.

I. INTRODUCTION

The interaction mechanisms between SAR backscatter and the structural properties of forests were the objects of several studies [1], [2]. Plant characteristics (e.g. density, orientation, shape, dielectric constant, height), soil conditions (wet, dry) and aspects of SAR imaging (polarization, incidence angle and wavelength) are important to determine the backscattered radiation to the SAR antenna. There are several interaction mechanisms of the radar signal with forest targets, such as: multiple backscatter within the canopy (volumetric scattering), direct scattering from the tree trunks, scattering from the interaction canopy-soil, scattering from the interaction trunk-soil (double bounce), whose intensities depend on the SAR wavelengths, on the polarization, on the angle of incidence and on terrain parameters. SAR data are also used to model forest biomass estimation, using the backscatter coefficient. Depending on the frequency of the sensor, there is a radar signal saturation for those areas with high biomass concentration. When the estimated biomass and the forest type are known, tree height and other forest parameters can be derived using allometric equations. Studying the configuration of σ^0 values, the penetration capacity and the predominant scattering mechanisms on vegetation as well as biomass evaluation from multi-frequency and multi-

polarized AIRSAR data, was verified that bands P_{HV} and L_{HV} are more sensitive to total biomass, presenting furthermore a strong relation with some structural forest parameters such as Height (H), Basal area (G), Density and Diameter (DBH) [3]. Nevertheless variations in the floristic composition, forest structure and management practices can have an important effect on the results [4]. The high correlation among biomass and L- σ^0_{HH} , saturated at 100ton/ha for both polarizations was found by [5] at a temperate coniferous forest. The same authors, using the decomposition of Freeman and Durden [6] generate a scattering model of each tree component, where volume scattering is around 80-90%, when the biomass exceeds 50 ton/ha. For younger stands the component of surface scattering is of around 20%, and the volumetric scattering components are below 70%.

The objective of this paper is to evaluate the interaction of L-band scattering with structural parameters from primary forest and secondary succession, including the effect of variations of the incidence angle at the moment of SAR imaging on the response of forest targets investigated. Additionally an analysis was made on the contribution of scattering mechanisms on the forest types studied, using the Freeman-Durden decomposition technique. The selected area under study is located in the region of Tapajós (Brazil), geographical coordinates S 3° 01' 59.85" to S 3° 10' 39.33" and WGr 54° 59' 53.08" to WGr 54° 52' 44.96".

II. MATERIAL AND METHODS

In this study we used polarimetric L-band SAR images, obtained during an airborne campaign with R99-B/SIPAM in September 2005, at HH, VV and HV polarizations (descending mode), spatial resolution of 5 m.. The SAR-R99 data were initially calibrated: 1st antenna pattern correction to remove gain variations in the range direction by a polynomial function applied to the sum of the amplitude values; and 2nd absolute calibration, based on the 12 corner reflectors placed in the area under study during the imaging campaign, to allow the transformation of amplitude data in backscatter values of targets, using the method of peak power [7]. For the absolute SAR calibration, the average error was -0.8443 dB and the standard deviation 0.18 dB. The σ^0 values at different polarizations were obtained taking

into account the average of pixels available at each ROI, corresponding to each one of the samples inventoried during field survey. At the SAR image, the ROI area includes the sample dimension with a sufficient amount of pixels representative for the theme, reducing so the statistical uncertainties and the influence of speckle noise [5].

The evaluation of the basic scattering mechanisms was done using the decomposition technique of Freeman-Durden [6], applied to complex images, which allows to estimate the absolute contribution from each one of these mechanisms (double-bounce, surface and volumetric). According to these authors the scattering contribution is obtained by the following expressions:

$$\langle |Shh|^2 \rangle = fs|\beta|^2 + fd|\alpha|^2 + fv$$

$$\langle |Svv|^2 \rangle = fs + fd + fv$$

$$\langle ShhSvv^* \rangle = fs\beta + fd\alpha + fv/3$$

$$\langle |Shv|^2 \rangle = fv/3$$

$$\langle ShhShv^* \rangle = \langle ShvSvv^* \rangle = 0.$$

where fv , fd and fs are the contributions to the power in VV polarization from volume, dihedral, and surface scattering, respectively. The coefficient α and β are the parameters that can be estimated from some forest variables, such as trunk radius and tree number density. Determining whether double bounce or surface scattering is the dominant contribution by using the sign of $\text{Re}(S_{HH} S_{VV}^*)$, according [8] enables us to identify the contribution of each scattering mechanism only from SAR polarization data, without any field data. Applying this technique we obtained the percent values of the scattering mechanisms over each of the sampled areas (ROI).

The biophysical parameters were collected in 5 areas of primary forest (each plot = 2,500 m²) and 8 areas of secondary succession (each plot = 1,000 m²), positioned geographically with a GPS. It is import to inform that measure of H and DBH, which allowed to generate the values of the basal area and biomass of the areas of secondary succession, were collected during 2002. In order to reduce the effect of the time imbalance between the field survey (2002) and the SAR imaging (2005), a correction factor was applied to the field inventory data, calculated on the average intervals of tree height and diameter. Such stratification was defined considering the height and DBH intervals from 3 m and 3 cm for the secondary succession respectively. This allowed to establish the average yearly increment by class of interval, considering the recovery age of each plot of secondary succession. The biomass estimation, specific allometric equations for primary forest [9] and secondary succession [10] were used.

III. RESULTS AND DISCUSSIONS.

3.1. Backscatter versus biophysical parameters

Table 1 presents an overview of the SAR characteristics referring to backscatter mechanisms for all primary forest (PF) and secondary succession (SS) samples, including its biophysical parameters. Those areas of primary forest

present $\sigma_{HH}^0 = -7.51 \text{ dB} \pm 3.34$, $\sigma_{HV}^0 = -12.25 \text{ dB} \pm 3.15$ and $\sigma_{VV}^0 = -7.53 \text{ dB} \pm 3.24$; secondary succession areas, which represent intermediate and advanced phases (characterized by the regeneration age and also by the vertical structure) present $\sigma_{HH}^0 = -7.38 \text{ dB} \pm 2.34$, $\sigma_{HV}^0 = -11.95 \text{ dB} \pm 2.27$ and $\sigma_{VV}^0 = -7.06 \text{ dB} \pm 2.29$. The values found in this study are coherent with those obtained by [4], [11], [12], whose variability can be attributed to general differences in the horizontal and vertical structure of the strata from the forest typologies. This also shows that the SAR-R99B presents an adequate radiometric response, if compared to those of other L- band SAR systems used, at the same polarizations.

The analysis of σ^0 , for both primary forest and secondary succession areas, shows that there are similar values for the co-polarizations and a stronger backscatter at VV and HH. The return signal is more reduced at the cross-polarization, which is more sensitive to volumetric scattering (random distribution of branches, twigs and leaves), that are not significant contributors for the total biomass. The relation between polarizations and biophysical parameters was evaluated by simple linear regressions. Table 2 shows the R² values and one verifies that the variable “tree height” presented solely the best relation with the σ_{HH}^0 when compared with the other biophysical variables.

Table 2. Determination coefficient (R²) among biophysical parameters and backscatter coefficients.

Variables	L-HH	L-HV	L-VV
Density (N ha ⁻¹)	0.0320	0.0037	0.0025
Basal area (m ² ha ⁻¹)	0.0654	0.0672	0.1186
Tree Heigh (m)	0.4380	0.3384	0.3276
Diameter (cm)	0.1106	0.0631	0.0500
Biomass (m ² ha ⁻¹)	0.0355	0.0541	0.1036

The analysis of backscatter of the 13 ROIs consider not only the physiognomic-structural characteristics of the forest types, but also the incidence angle (Θ) of the imaging. Since the imaging swath of the SAR R99-B was of 30 Km, and the incidence angle varies between 52.7 a 70.1°, the sampled plots are located, from near to far range between 57° and 65° (Table 1). There is a strong tendency of increasing σ_{hh} with the increment of the Θ value, which contradicts the thesis that at grazing angles the specular reflexion would predominate. A possible explanation for this phenomenon is related to the radar wavelength, the most relevant volumetric scattering and double-bounce mechanisms, taking into account the higher penetration capacity of L band in the different strata of primary or secondary forest.

Due to the importance of the incidence angle (Θ) the evaluation of backscatter was also done together with the biophysical parameters (Table 3) by multiple regression. The choice of the parameters was made considering the correlation matrix of the total from independent variables, jointly with the construction model for the multiple

regression of Best subsets, based on choice criteria R^2 , R^2 adjusted and Mallows' C_p . Based on the mentioned statistical test, the backscatter are best explained by the vertical structure (log H) of the forest type and by the incidence angle. For a 90% level of trust, the best fit was obtained for polarization HH ($R^2 = 0.59$).

Table 3 Relation model between backscatter and tree height, including the SAR incidence angle. The values in red are significant due to the p-value, at a 90% level of trust.

$\alpha = 0.10$		$y = a + b \log(H) + c(\Theta)$			
		a	b	c	R^2
σ^0	HH	-22.4537	2.7171	0.1330	0.59
	p-Value		0.0882	0.1035	
	HV	-26.7827	2.4601	0.1387	0.50
	p-Value		0.1782	0.1446	
	VV	-23.3894	2.0736	0.1784	0.56
	p-Value		0.2307	0.0592	

An additional analysis on the influence of the vertical structure (height class intervals) from the forest cover and of the incidence angle (Θ) on the Sigma Nough (σ^0) values was done in this study. At Figure 1 one observes an example of tree stratification by height intervals for three samples of primary forest. Considering the configuration of these samples, they present all a similarity on the distribution of trees by strata. For those cases of very close incidence angles, the backscatter values at different polarizations are quite similar. This fact does not occur when there are differences at the imaging angle, with a significant increase on the σ^0 values at higher incidence angles.

3.2. Contribution of the scattering mechanisms.

Using the Freeman-Durden decomposition, it was possible to verify the contribution of the three components of the scattering mechanism (surface, double-bounce and volumetric) for each one of the ROIs, representing primary forest and the secondary succession stages. The model indicated (Figure 2) that volume scattering is a dominant component and accounts for 93.71 - 95.74% of the total scattering, on both primary forest types and intermediate/advanced recovery stages. Double-bounce scattering components present values between 1.14 - 2.19% of the total scattering and the surface scattering corresponds to 2.86 - 4.11% of the total. It is important to mention that the surface scattering fraction presents values slightly above those of the double-bounce component. The inversion of the performance from these two last scattering mechanisms, specifically in tropical forests, can be due to high incidence angles (Θ), because higher incidence angles favor the specular reflexion.

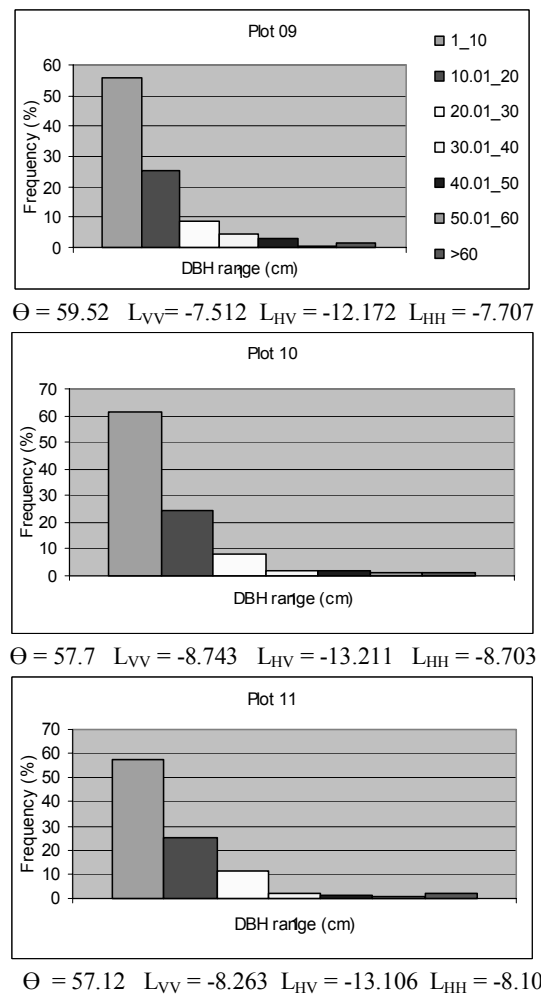


Figure 1. Diagram of primary forest strata and respective backscatter values associated to the SAR incidence angles.

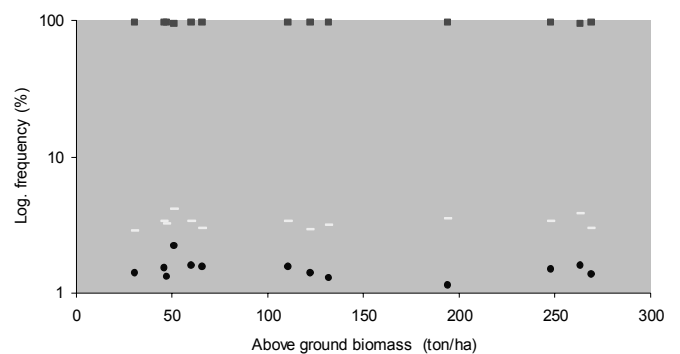


Figure 2. Contributions of three scattering components (volume: square; surface: line; double-bounce: circle) for a primary forest plotted against biomass.

IV. CONCLUSIONS

The L-band σ^0 values for three polarization modes (HH, VV and HV) from SAR R99-B/SIPAM were obtained at 13 sites of primary forest and secondary succession, in parallel with ground measurements. The relationship of SAR data and biophysical variables can be summarized as follows:

1. for similar structural conditions the primary or secondary forest cover can present different backscatter if the sampled areas are within an imaging track with variations of the incidence angle;
2. the variable height has a better performance to explain the backscatter, when compared to other biophysical variables;
3. using a simple decomposition model, the component of volumetric scattering mechanism has a stronger influence on the SAR response of primary and secondary tropical forest.

The preliminary results of this study indicate that multi-polarized SAR-R99 images, allows to understand the effects of the structural aspects at the radar response, confirming that this is a very important experiment to characterize and monitor the Amazon landscape.

ACKNOWLEDGMENT

Thanks to CENSIPAM and LBA. The research was also funded by research grants provided by CNPq, CAPES.

REFERENCES

- [1] I. Champion, D.Guyon, J.Riom, "Effect of forest thinning on the radar backscattering coefficient at L-band", *International Journal of Remote Sensing*, vol.19, n.11, p. 2233-2238, 1998.
- [2] T. Neeff, L.V. Dutra, J.R. Santos, C.C. Freitas, L. S. Araújo, "Power spectrum analysis of SAR data for spatial forest characterization in Amazônia", *International Journal of Remote Sensing*, vol., 26, n.13, p. 2851-2865, 2005.
- [3] E. Mougin, C. Proisy, G. Marty, F. Fromard, H. Puig, J.L. Betoulle, J.P. Rudant, "Multifrequency and Multipolarization Radar Backscattering from Mangrove Forests", *IEEE Transactions on Geoscience and Remote Sensing*, vol. 37, n.1, p. 94-102, 1999.
- [4] D.H. Hoekman, M.J. Quiñones, "Land cover type and biomass classification using Air SAR data for evaluation of monitoring scenarios in the Colombian Amazon", *IEEE Transactions on Geoscience and Remote Sensing*, vol.38, n.2, p. 685-696, 2000.
- [5] M. Watanabe, M. Shimada, A. Rosenqvist, T. Tadono, M. Matsuoka, A.A. Romshoo, K. Ohta, R. Furuta, K. Nakamura, T. Moriyama, "Forest structure dependency of the relation between L-Band σ^0 and biophysical parameters", *IEEE Transactions on Geoscience and Remote Sensing*, vol. 44, n.11, p. 3154-3165, 2006.
- [6] A. Freeman, S.L.A. Durden, "Three component scattering model for polarimetric SAR data", *IEEE Transactions on Geoscience and Remote Sensing*, vol.36, n.3, p. 963-973, 1998.
- [7] A.L. Gray, P.W. Vachon, C.E. Livingstone, T.L. Lukowski,, "Synthetic Aperture Radar calibration using reference reflectors", *IEEE Transactions on Geoscience and Remote Sensing*, vol.,28, n. 3, p.374-383, 1990.
- [8] J. J. van Zyl, "Unsupervised classification of scattering behavior using radar polarimetry data", *IEEE Transactions on Geoscience. and Remote Sensing*, vol. 27, p. 36-45, 1989.
- [9] S. Brown, A.J.R. Gillespie, A. E. Lugo, "Biomass estimation methods for tropical forest with applications to forest inventory data", *Forest Science*, vol. 35, p.881-902, 1989.
- [10] C. Uhl, R. Buschbacher, E.A.S. Serrão, "Abandoned pastures in eastern Amazonia, I: patterns of plant succession", *Journal of Ecology*, vol.76, p. 663-681, 1998.
- [11] S.S. Saatchi, J.V. Soares, D.S. Alves, "Mapping deforestation and land use in Amazon rainforest by using SIR-C imagery", *Remote Sensing of Environment*, vol.59, p. 191-202. 1997.
- [12] J.R. Santos, M.S. Pardi.Lacruz, L.S. Araujo, M. Keil, "Savanna and tropical rainforest biomass estimation and spatialization using JERS-1 data", *International Journal of Remote Sensing*, vol.23, n.7, p. 1217-1229, 2002.

Table 1. Incoherence and coherence parameters of SAR L-band for sites and respective biophysical parameters of forest typologies.

Plots	G (m ² /ha)	H (m)	Density (n° ind./ha)	Biomass (ton/ha)	N° pixels	Θ	σ vv	Stdev	σ hv	Stdev	σ hh	Stdev	Scattering components			
													Pd (dB)	Pv (dB)	Ps (dB)	
SS	1	14.11	10.14	920	60.21	3276	57.38	-9.698	2.640	-14.423	2.603	-9.395	2.665	-33.233	-15.459	-29.952
	2	15.54	11.10	1510	66.17	3710	58.17	-6.622	2.161	-11.462	2.114	-6.968	2.196	-32.510	-14.608	-29.747
	3	11.87	11.81	1040	51.32	3078	63.64	-6.948	2.437	-12.714	2.277	-8.319	2.439	-33.979	-17.665	-31.249
	4	11.07	11.66	1160	47.53	3021	63.48	-6.835	2.103	-11.633	2.269	-6.916	2.264	-33.233	-15.459	-29.952
	5	10.34	12.75	980	46.23	3325	65.54	-6.295	2.204	-10.903	2.128	-6.268	2.305	-34.698	-16.691	-31.221
	6	6.61	12.52	630	30.96	6902	60.41	-6.786	2.114	-11.532	2.063	-7.217	2.112	-32.950	-14.557	-29.801
	7	21.08	15.38	1228	111.00	6811	60.25	-6.504	2.344	-11.407	2.345	-6.973	2.359	-33.010	-15.134	-29.690
	8	27.00	13.85	452	131.99	3923	60.29	-6.779	2.357	-11.490	2.377	-6.983	2.380	-33.862	-15.147	-29.987
PF	9	32.38	12.01	1176	269.37	6883	59.52	-7.512	3.095	-12.172	3.036	-7.707	3.192	-32.741	-14.336	-29.446
	10	29.44	11.29	1220	248.16	3129	57.7	-8.743	3.279	-13.211	3.153	-8.703	3.418	-32.197	-14.133	-28.713
	11	29.88	12.72	420	263.32	2131	57.12	-8.263	3.244	-13.106	3.124	-8.100	3.249	-32.823	-15.023	-29.031
	12	18.74	17.81	432	194.33	3603	65.72	-6.301	3.162	-11.122	3.079	-6.161	3.314	-36.198	-16.990	-31.349
	13	14.53	15.79	460	122.60	5441	62.91	-6.812	3.412	-11.633	3.362	-6.868	3.534	-34.179	-15.792	-31.024